J. exp. Biol. **162**, 231–249 (1992)
Printed in Great Britain © *The Company of Biologists Limited 1992*

ELECTRICAL RESPONSES TO CHEMICAL STIMULATION OF SQUID OLFACTORY RECEPTOR CELLS

BY MARY T. LUCERO, FRANK T. HORRIGAN AND WM F. GILLY
Hopkins Marine Station, Stanford University, Pacific Grove, CA 93950, USA

Accepted 19 August 1991

Summary

Electrical properties of isolated olfactory receptor cells were studied using voltage- and current-clamp techniques based on whole-cell patch-clamp methods. Squid olfactory receptor cells contain voltage-gated Na^+ and K^+ channels and are capable of generating action potentials. Chemicals that elicit escape-jetting responses in behavioral experiments affect the excitability of isolated receptor cells. One set of such chemicals, including quaternary ammonium ions and aminopyridines, blocks K^+ channels and increases excitability. Squid ink and L-Dopa also elicit escape jetting, but these substances increase membrane conductance, hyperpolarize the receptor cell and decrease excitability. These experiments indicate that sensory neurons of the olfactory organ are capable of detecting chemical signals and that at least two different transduction mechanisms can lead to similar behavioral responses.

Introduction

Anatomical studies have shown that squids (and other cephalopods) have what is termed an 'olfactory organ' generally located posterior and ventral to each eye (Watkinson, 1909; cited by Emery, 1975; Wildenburg and Fioroni, 1990). This olfactory organ is the site of a sensory epithelium composed of ciliated support cells and several types of putative receptor cells. The receptor cells are bipolar neurons that send an apical dendritic stalk to the surface of the olfactory organ where the specialized sensory cilia are exposed to the ambient sea water. A small unmyelinated axon leads from the basal surface of each receptor neuron to the 'olfactory lobe' and other areas of the brain (Messenger, 1979). Within the brain, afferent tracts from the olfactory lobe impinge on motor centers that control swimming and escape jetting and on the optic gland, a structure thought to affect gonadal maturation (Wells and Wells, 1959). The anatomy thus suggests links between chemoreception and escape jetting as well as sexual or reproductive activity.

It is surprising, given these anatomical studies describing structures and pathways so similar to their likely counterparts in vertebrate olfactory systems,

Key words: cephalopod, squid, *Loligo opalescens*, chemoreception, olfaction, patch-clamp, ion channels, L-Dopa.

that behavioral or physiological studies on the squid olfactory system have been so limited. Our behavioral study (Gilly and Lucero, 1992) provides the first evidence for chemoreception of water-borne chemical signals by the olfactory organ in squid.

In the present study, we extend the behavioral work (Gilly and Lucero, 1992) to the receptor cell level. Primary receptor neurons isolated from the squid olfactory organ contain voltage-gated Na^+ and K^+ channels and are capable of generating repetitive action potentials. When tested on isolated receptor cells, chemicals that cause escape jetting fall into two categories. Chemicals in one category block K^+ channels, depolarize the cell and increase excitability. Such blockers include quaternary ammonium ions and 4-aminopyridine (4-AP). The second category includes squid ink and L-Dopa, both of which act in the opposite way to increase membrane conductance, hyperpolarize the cell and decrease excitability. Thus, it appears that squid olfactory receptor cells convey sensory information about certain chemicals in their environment by at least two mechanisms that change the firing pattern of the receptor cells. A preliminary report of this work has appeared in abstract form (Lucero *et al.* 1991).

Materials and methods

Dissection of olfactory organ and culture conditions

The olfactory organ of adult *Loligo opalescens* Berry was excised under a dissecting microscope and treated with non-specific protease (10 mg ml^{-1} Sigma type XIV) in sterile filtered sea water at 18–20 °C for 50 min. Following a 3–5 min rinse in fresh filtered sea water, the isolated olfactory organ was placed on a nylon screen (100 μm mesh size) in a tissue culture medium consisting of Leibovitz's L-15 (Gibco, Inc) supplemented with 263 mmol l^{-1} NaCl, 4.64 mmol l^{-1} KCl, 9.05 mmol l^{-1} $CaCl_2$, 49.54 mmol l^{-1} $MgCl_2$, 2 mmol l^{-1} Hepes (pH 7.8), 2 mmol l^{-1} L-glutamine, 50 i.u. ml^{-1} penicillin G and 0.5 mg ml^{-1} streptomycin. The olfactory organ remained relatively intact with this treatment and was incubated at 16–17 °C for periods ranging from 1 h to 2 days before use in electrophysiological experiments.

Whole-cell and nystatin patch recordings

Isolated olfactory cells were obtained for electrophysiological study by removing the nylon screen and adherent olfactory organ from the culture dish with sterile forceps and dipping the screen into the bath solution in the glass-bottomed experimental chamber (100 μl volume). Cells were allowed to settle for about 5 min before the chamber was thoroughly flushed to remove debris and non-adherent cells. Experiments were conducted at 10 °C.

The solution surrounding the cells was changed either in bulk by superfusing the entire chamber or focally from a small pipette. For the focal solution changes an automated micromanipulator (Eppendorf 5170 and 5242 microinjector, Madison, WI) was used to lower a 'puff' pipette approximately 10 μm in diameter filled with

test solution and 1 mmol l^{-1} blue no. 1 (Brilliant Blue) dye. It took the pipette 0.5 s to travel from the surface of the bath to the bottom of the chamber. The pipette was positioned approximately 50 μm from the apical portion of the cell. To ensure that bath solution was not unintentionally drawn up into the puff pipette, 10–20 kPa of pressure was applied immediately before entering the bath. Thus, test solution was ejected during the entire time (8–15 s) that the pipette was in the bath. Control and test substances were applied either through the same pipette, by pulling bath solution into the pipette after a test run, or by using a multibarrelled pipette. Complete removal of the pipette from the bath also took 0.5 s.

For whole-cell recordings (Hamill *et al.* 1981), electrodes were pulled from either KG12 or 0010 glass (Garner Glass, Claremont, CA), coated with Sylgard (Dow Corning, Midland, MI), and had resistances of 1–2 MΩ when filled with an internal solution. To establish the whole-cell recording configuration, the electrode was pressed against the cell while tip resistance was being monitored. Once a high-resistance seal had formed ($>10^9\,\Omega$), the holding potential was set to -70 mV, and gentle suction was applied to rupture the membrane under the pipette. An advantage of this conventional whole-cell technique is that macroscopic currents can be studied while controlling the cell's internal solution. A disadvantage is that second messenger systems are washed out of the cell.

The nystatin 'perforated' patch technique (Horn and Marty, 1988) was also used to examine cells under voltage- and current-clamp, presumably with second messenger systems more intact. In these experiments, a thick-walled (0.64 mm) Boro-glass pipette with a capillary filament (Sutter Instrument Co., Novato, CA) was back-filled with 50 μg ml^{-1} nystatin internal solution. Positive pressure was applied to the patch electrode during the descent through the bath. Just before touching the cell, the pressure was released and the pipette current was balanced to zero. Upon touching the cell, gentle suction was applied to the patch electrode only until a high-resistance seal formed between glass and cell. The holding potential was set to -70 mV. Within 10 min the electrical transient associated with the cell's input capacitance grew larger and faster, indicating that nystatin pores had formed to allow electrical access to the cell interior.

25–65 % of the resistance in series with the cell membrane was compensated for by positive feedback. Linear leak currents and the small residual, uncompensated capacity currents were subtracted on-line using a 'P/4 procedure' (Armstrong and Bezanilla, 1974). All voltage-clamp records presented in this paper have been leak subtracted. Averages are presented as the mean$\pm$1 standard error. Holding potential was always -70 mV.

Data acquisition

Voltage-clamp and current-clamp experiments were run using either a 125 kHz DMA Labmaster/TL-1-125 Interface (Axon Instruments, Foster City, CA) and a Zenith 386 computer or a custom-built interface and a DEC 1123 computer (Gilly and Brismar, 1989). Membrane voltages and currents were measured using a List-EPC7 (Adams and List, Great Neck, NY) amplifier, sampled with a 12-bit A/D

converter at a sample rate of 1.3–100 kHz and filtered at 3–10 kHz. Continuous recordings in current-clamp mode were recorded on a Toshiba digital hi-fi VHS DX900 using PCM (Unitrade, New York) with a sample rate of 44.1 kHz and played back through the Labmaster/TL-1-125 for further analysis.

Solutions and channel blockers

Compositions of external bath and internal pipette solutions for the different experiments are given in each figure legend. Internal solutions were buffered to pH 7.2, and bath solutions were buffered to pH 7.4 with Hepes. For nystatin patch experiments, a nystatin stock solution of 25 mg ml^{-1} in dimethylsulfoxide was made daily and added to the filtered internal solution. All chemicals were obtained from Sigma Chemical Co. (St Louis, MO).

Tetramethylammonium (TMA^+), tetraethylammonium (TEA^+), tetrabutylammonium (TBA^+) and 4-aminopyridine (4-AP) were added in powdered form to the appropriate external artificial sea water (ASW). Methadone was made up as a 100 mmol l^{-1} stock solution in ASW and diluted to 500 μmol l^{-1} just prior to use. L-Dopa was added in powdered form to ASW, sonicated for 2 min, and used within 2 h. Squid ink extract was prepared by placing a cut open ink sack in 1 ml of ASW, vortexing it for 2 min, centrifuging at 14 000 *g* for 2 min and filtering the supernatant through a 0.2 μm filter. This extract, hereafter referred to simply as 'ink', was freshly prepared on the day of use.

Results

Receptor cell morphologies

Fig. 1A–C shows examples of living olfactory organ cells that have been freshly dissociated. Several kinds of putative chemoreceptor cells are recognizable, and the morphologies to be described persist for 1–2 days *in vitro*. The most common type (Fig. 1A) is termed pyriform and has a long axonal process arising from the basal pole containing the nucleus and a spike-like process that projects from the apical pole. Most of the cell body appears to be filled with granular material or cristae, and the bulk of the cell's 'interior' is actually an invaginating extracellular cavity filled with cilia (Emery, 1975). These cells appear equivalent to the 'Type 4' receptors described on ultrastructural grounds in *Lolliguncula brevis* (Emery,

Fig. 1. Acutely dissociated receptor cells from the olfactory organ. (A–C) Light micrographs of living cells in culture medium. (A) The most common type of cell is pear-shaped (pyriform). Pyriform cells are distinguished by the large cilia-filled invaginating pocket, the basal nucleus (*n*) and the single spike-like structure on the apical pole (arrow). An axon (*ax*) arises from the basal pole. (B) Floriform cells have a smaller soma with a long thin neck that swells to form a petaloid arrangement of the apical cilia. (C) Cells intermediate in appearance between pyriform and floriform cell types also exist. The example illustrated here has a spike-like apical process and a constricted neck. (D) Scanning electron micrograph of a floriform cell; (E) scanning electron micrograph of a pyriform cell; (F) scanning electron micrograph of an enlarged floriform knob. Scale bars, A–C, 10 μm; D,E, 5 μm; F, 1 μm.

1975). A low-power scanning electron micrograph of an aldehyde-fixed pyriform receptor (see Materials and methods in Gilly and Lucero, 1992) is shown in Fig. 1E; the spike-like process is evident.

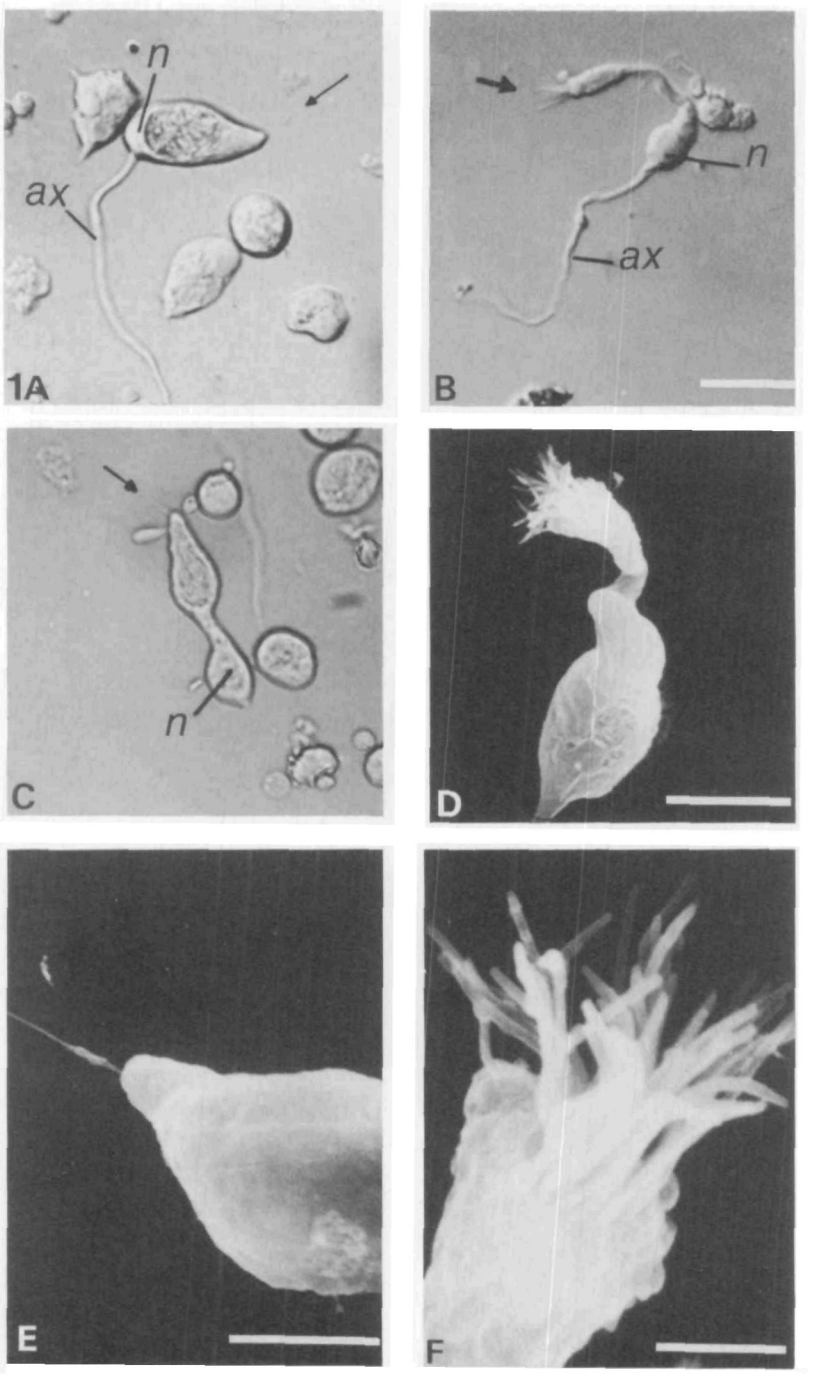

A second distinctly different receptor cell type is termed floriform (Fig. 1B). This type also displays a prominent axonal process, but in this case a long, thin neck extends from the cell body and is crowned by a swelling covered with non-motile cilia arranged in a petaloid fashion. Such floriform cells are probably those Emery labeled Type 2 or Type 5 receptors. Fig. 1D,F shows scanning electron micrographs of a fixed floriform receptor. Pyriform and floriform receptor cells were the most distinctly identifiable and most common types of cells. Electrophysiological experiments were conducted on both.

A third, less common receptor may be related to the pyriform-type cell on the basis of the presence of a 'spike-like process' on the apical pole (Fig. 1C). In this type of cell, however, the portion of the cell body containing the nucleus is separated by a short neck from the apical swelling filled with cilia and granular material. This type of receptor appears to be equivalent to Emery's Type 3.

Passive properties of floriform and pyriform receptor cells

Resting potentials were determined in receptor cells immediately after obtaining electrical access to the cell's interior, with the whole-cell electrode measuring voltage (current-clamp mode). Pyriform receptors have a mean resting potential of -58.2 ± 1.2 mV (N=91). Floriform cells have less negative resting potentials that are not stable and generally fluctuate rapidly from -50 mV to -25 mV (N=5). Thus, we were not able to obtain a meaningful average value of the floriform cell resting potential. Resting potential data are also displayed in Table 1 (measured with 400–450 mmol l^{-1} K^+ in the pipette).

Passive electrical properties of voltage-clamped floriform and pyriform receptor cells were examined by applying voltage steps from the holding potential of -70 mV to -120 mV. No voltage- or time-dependent currents were activated in this voltage range. The mean values for input resistances, input capacitances and

Table 1. *Passive membrane properties of single receptor cells of the olfactory organ*

Cell type	Resting potential (mV)	Input resistance (MΩ)	Input capacitance (pF)	Capacity current time constant	
				Fast (μs)	Slow (ms)
Pyriform	−58.2+1.2	406+77	11.9+1.0	78+6	1.7+0.2
(N)	(91)	(30)	(40)	(16)	(16)
Floriform	−25 to −50	1700+400	5.7+0.5	88+8	–
(N)	(5)	(14)	(11)	(14)	

Means±1 S.E. are given; the number of cells (N) is also indicated.

Input capacitance refers to the fast component only for pyriform cells; it was determined after the slow component had vanished (see text for additional details).

The resting potentials of all floriform cells studied were very unstable, hence the range of observed values.

time constants for the capacity current transients measured from both pyriform and floriform cells are listed in Table 1. The highest input resistance measured for a floriform receptor of 5.4 GΩ was considerably higher than the maximum of 1.8 GΩ in a pyriform receptor cell.

Input capacitance of pyriform cells was larger than that in floriform cells, and pyriform cell capacity current transients showed both fast and slow components with time constants of 78±6 μs and 1.73±0.17 ms, respectively (N=16). The slow component sometimes suddenly disappeared during an experiment with no change in the amplitude of the fast component. This phenomenon often occurred after 15 min or so and is almost certainly associated with loss of electrical access to the large invaginating cavity in the interior of the cell. Voltage-dependent currents under study at the time were not obviously altered by this event. The average value of input capacitance after loss of the slow component was 11.9±1.0 pF (N=40).

Sodium currents

Both pyriform and floriform receptor cells are excitable and contain a complement of ion channels similar to those found in other squid neurons (Brismar and Gilly, 1987; Gilly and Brismar, 1989). Na^+ currents sensitive to tetrodotoxin (TTX) (obtained by subtracting voltage-clamp records obtained in the presence of 100 nmol l^{-1} TTX from those recorded in the absence of drug from the same cell) are illustrated in Fig. 2A. These currents were elicited by voltage steps to −40 mV and beyond (10 mV increments to +70 mV) from a pyriform cell bathed in a zero-potassium artificial sea water (ASW) and internally dialyzed with a Na^+-containing internal solution. The conductance–voltage relationship calculated by dividing the peak current at each potential by the driving force shows that the channels first activate near −30 mV and reach a half-maximal conductance at −5 mV (Fig. 2B). Inactivation of Na^+ current is steeply voltage-dependent between −50 and 0 mV and is half-maximal at approximately −25 mV (data not illustrated).

Na^+ currents recorded from a floriform cell under the same conditions are shown in Fig. 2C. The properties of the floriform cell Na^+ conductance (Fig. 2D) are similar to those observed in the pyriform cells. A major difference between cell types lies in the amplitude of the currents. The voltage-gated Na^+ currents in pyriform cells are about five times larger than those in floriform cells. Based on capacitance measurements (Table 1), a pyriform cell is only about twice as large as an average floriform cell.

Potassium currents

Other experiments were designed to study voltage-dependent K^+ currents (i.e. Na^+-free internal solutions with external TTX), and a series of currents recorded between −30 and +70 mV from a pyriform receptor cell is illustrated in Fig. 3A. Outward currents activate between −30 and −20 mV and show a marked, voltage-dependent delay. Analysis of shifts in reversal potential with changing external K^+

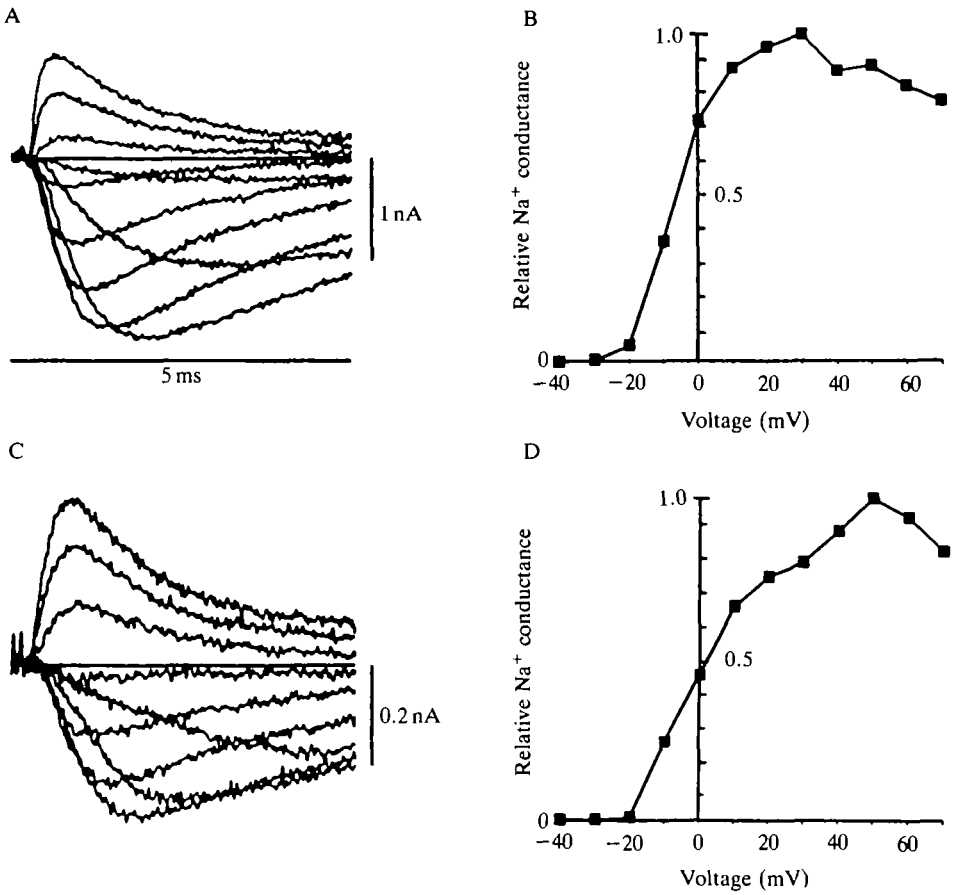

Fig. 2. Voltage-gated Na^+ currents are found in both pyriform and floriform olfactory receptor cells. (A) Superimposed TTX-subtracted Na^+ currents from a pyriform cell rapidly activate and inactivate during 5 ms voltage steps. (B) Relative Na^+ conductance is plotted from the data in A. (C) Na^+ currents from a floriform cell recorded using the same voltage protocol as in A are similar to, but smaller than, Na^+ currents in pyriform cells. (D) The conductance–voltage relationship for the floriform Na^+ currents in C reveals similar voltage dependence of Na^+ channel activation in the pyriform cell. Zero-K^+ bath solution: 480 mmol l^{-1} NaCl, 50 mmol l^{-1} $MgCl_2$, 10 mmol l^{-1} $CaCl_2$, 10 mmol l^{-1} Hepes. Internal solution: 50 mmol l^{-1} NaCl, 100 mmol l^{-1} sodium glutamate, 50 mmol l^{-1} NaF, 300 mmol l^{-1} tetramethylammonium glutamate, 25 mmol l^{-1} TEACl, 10 mmol l^{-1} EGTA, 10 mmol l^{-1} Hepes.

concentrations indicates that these currents are carried by K^+-selective channels (not illustrated). The kinetic properties evident in Fig. 3A and the voltage-dependence of the peak K^+ conductance (Fig. 3C) are very similar to analogous data obtained in squid giant axon or giant fiber lobe (GFL) neurons of the stellate ganglion (Llano and Bookman, 1986). As in GFL cells, the K^+ currents in pyriform receptors partially inactivate during a long depolarization (Fig. 3B).

Floriform receptor cells also have voltage-dependent K^+ currents that are

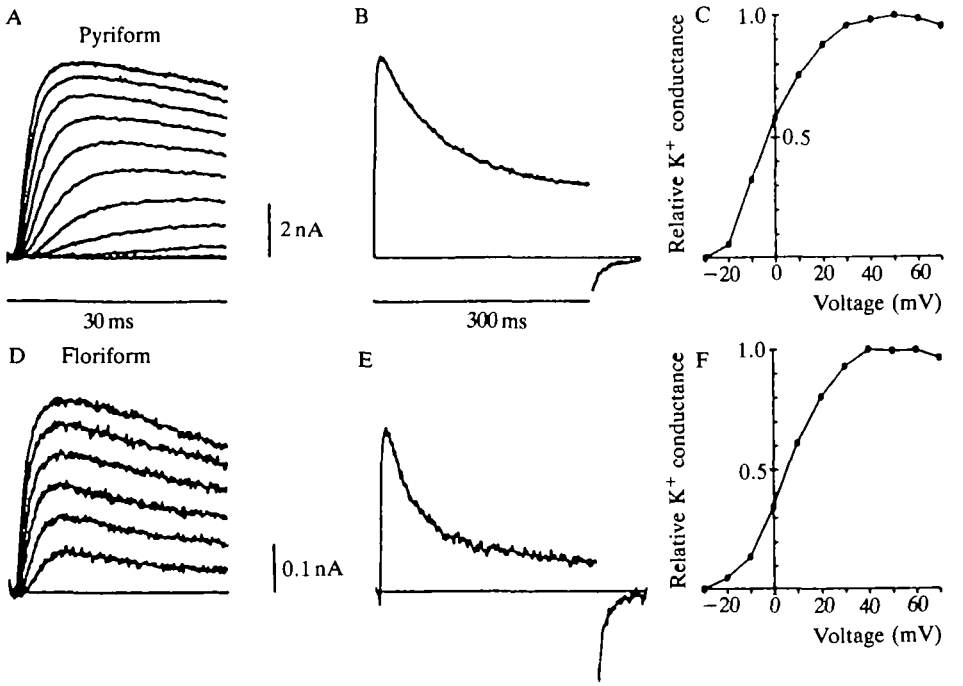

Fig. 3. Delayed rectifier K^+ currents from pyriform and floriform cells have similar kinetics but differ in amplitude. (A,D) Outward K^+ currents activate with a delay in response to 30 ms voltage steps to levels between −30 mV and +70 mV (10 mV increments) in a pyriform cell (A) and a floriform cell (D). Note the difference in scale bars between the two cell types. (B,E) K^+ current inactivates during a long (300 ms) pulse to +70 mV. Inactivation is slightly greater and more rapid in the floriform cell (E) than in the pyriform cell (B). (C,F) Relative K^+ conductance is plotted from the data in A and D, respectively. K^+ currents from both cell types activate between −30 and −20 mV and reach a half-maximal conductance between −5 and +10 mV. Artificial sea water bath solution: 470 mmol l^{-1} NaCl, 10 mmol l^{-1} KCl, 50 mmol l^{-1} $MgCl_2$, 10 mmol l^{-1} $CaCl_2$, 10 mmol l^{-1} Hepes, (plus 100 nmol l^{-1} TTX). 100K internal solution: 50 mmol l^{-1} KCl, 50 mmol l^{-1} KF, 350 mmol l^{-1} tetramethylammonium glutamate, 10 mmol l^{-1} EGTA, 10 mmol l^{-1} Hepes.

qualitatively similar to, but again consistently smaller than, those in pyriform cells (Fig. 3D–F). In this case, however, the kinetics of inactivation are slightly more rapid than those in pyriform cells (Fig. 3E).

Calcium currents

Although the majority of the voltage-dependent membrane currents in olfactory receptor cells are carried by Na^+ and K^+, some cells also have what appears to be a Ca^{2+} conductance. Experiments were designed to examine Ca^{2+} currents by replacing all external Na^+ and K^+ with *N*-methyl-D-glucamine, replacing internal K^+ with TMA^+ and TEA^+, and adding 50 mmol l^{-1} Ca^{2+} or Ba^{2+} plus 100 nmol l^{-1} TTX to the external solution. Under these conditions, a small,

voltage-dependent inward current (maximum peak current of 180 pA) was observed that was blocked by 2 mmol l^{-1} Cd^{2+}. This presumptive Ca^{2+} current was labile and disappeared after approximately 5 min; thus, there was little recovery of inward current after washout of Cd^{2+} (data not shown).

Action potentials in current-clamped receptor cells

Isolated olfactory receptor cells are capable of generating action potentials (APs) when current-clamped using either conventional whole-cell or nystatin-patch techniques. In Fig. 4A, current steps to subthreshold voltages elicit passive membrane voltage responses in a pyriform cell. Larger current pulses bring the membrane voltage to threshold and elicit trains of action potentials. Measurements made from the data illustrated in Fig. 4A reveal an AP threshold voltage of −31 mV, a peak amplitude of +55 mV (measured from threshold) and a duration at half-peak amplitude of 1.9 ms. These APs are generated by voltage-dependent Na^+ channels and are blocked by 100 nmol l^{-1} TTX (not illustrated). There is no obvious plateau phase, and it appears that Ca^{2+} channels probably play a minor role in shaping the AP. This is consistent with the very small Ca^{2+} currents seen under voltage-clamp conditions. Repolarization of the AP involves the delayed rectifier K^+ channels (see also below).

Repetitive firing was regularly observed in all pyriform cells with high-input resistance values, and some cells fired action potentials spontaneously without any injected current. Rates of spontaneous and induced firing varied in cells from 0.08 to 17.00 Hz. Some pyriform cells fired bursts of APs; others fired continuous

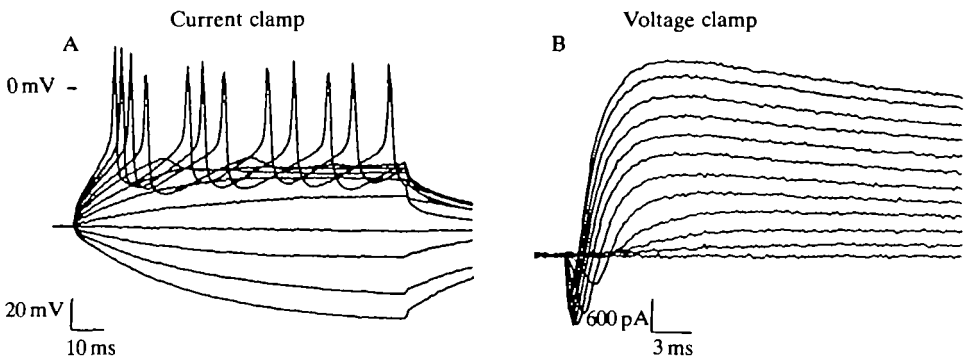

Fig. 4. Isolated olfactory receptor cells are capable of generating action potentials. (A) Voltage traces obtained from a pyriform cell (resting membrane potential of −64 mV) show repetitive firing upon reaching a threshold near −30 mV. Current pulses were applied for 100 ms in 50 pA increments from −200 pA to +400 pA. (B) Voltage-clamp measurements on the same cell reveal both inward Na^+ and outward K^+ currents during voltage steps between −50 and +60 mV. Bath solution: ASW (see Fig. 3). Potassium–nystatin internal solution: 20 mmol l^{-1} KCl, 380 mmol l^{-1} potassium aspartate, 10 mmol l^{-1} EGTA, 10 mmol l^{-1} Hepes, 100 mmol l^{-1} glucose, 50 μg ml^{-1} nystatin.

trains. Only a few presumably damaged cells, with input resistances of 100 MΩ or less, showed a single action potential regardless of the amplitude or duration of the current pulse stimulus. Data from such cells were not analyzed further.

Although floriform cells have voltage-gated Na^+ channels and produce a single action potential in response to electrical stimulation, the membrane potential fluctuates dramatically in current-clamp and trains of action potentials were not observed. Thus, the majority of work on floriform cells was carried out in voltage-clamp.

Voltage- and current-clamp experiments can be performed on the same cell. Fig. 4B shows a family of current traces (from the cell used in Fig. 4A) for voltage steps to levels between −50 and +60 mV. Both inward Na^+ and outward K^+ currents flow with the high-K^+–nystatin internal solution. There are no obvious differences between Na^+ and K^+ currents obtained with the nystatin method and those recorded with conventional whole-cell dialysis. The ability to examine both membrane currents and action potentials in the same cell is very useful when studying the mechanisms of chemosensory transduction.

Effects of channel-blocking compounds on isolated receptor cells

As the next step in studying the mechanisms involved in transducing chemical signals by squid olfactory cells, the effects of agents that elicited strong behavioral responses *in vivo* (Gilly and Lucero, 1992) were examined on isolated receptor cells. The first chemical tested was propyl paraben, a preservative in blue food coloring that caused escape jetting in behavioral tests (Gilly and Lucero, 1992). When bath-applied to isolated floriform or pyriform receptor cells 100 μmol l^{-1} propyl paraben reversibly blocked about 50 % of the peak K^+ current and 20 % of the peak Na^+ current (data not shown). This finding led us to test the effects of better-known K^+ and Na^+ channel blockers on squid escape jetting and on the electrical properties of receptor cells.

In an examination of three related quaternary ammonium compounds: tetramethyl-, tetraethyl- and tetrabutylammonium (TMA^+, TEA^+ and TBA^+, respectively), our behavioral studies showed that, although TMA^+ produced little behavioral effect, both TBA^+ and TEA^+ reliably elicited escape responses. In the present electrophysiological studies, we found that TBA^+ and TEA^+ blocked K^+ currents in isolated pyriform receptor cells, whereas TMA^+ did not.

Fig. 5 shows results from a voltage-clamp experiment in which 'puff' application (see Materials and methods) of 20 mmol l^{-1} TBA^+ blocked approximately 20 % of the K^+ current in a pyriform cell during a pulse to +40 mV (Fig. 5A), without affecting inward Na^+ current. The average block of peak K^+ current at +60 mV by bath-applied TBA^+ (20 mmol l^{-1}) was 52±9 % (N=5).

20 mmol l^{-1} TEA^+ also blocked K^+ currents when puff-applied to isolated pyriform receptor cells during a pulse to +40 mV without affecting Na^+ currents (Fig. 5B). Bath application of 20 mmol l^{-1} TEA^+ blocked 19±3 % (N=4) of the peak K^+ currents elicited during a pulse to +60 mV. 20 mmol l^{-1} TMA^+ essentially had no effect on either Na^+ or K^+ currents (Fig. 5C).

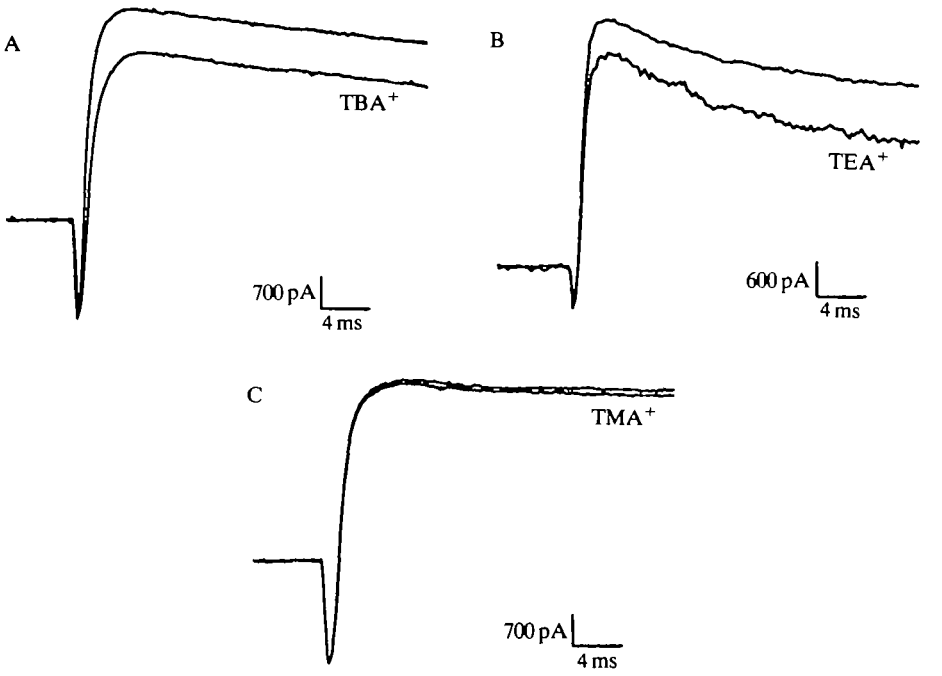

Fig. 5. Quaternary ammonium compounds reduce K^+ current without affecting Na^+ current in isolated pyriform cells. (A) 20 mmol l^{-1} TBA^+ blocks approximately 20 % of the outward K^+ current at +40 mV but has no effect on inward Na^+ current. (B) In a different cell, 20 mmol l^{-1} TEA^+ blocks approximately 15 % of the outward K^+ current at +40 mV but has no effect on inward Na^+ current. (C) 20 mmol l^{-1} TMA^+ has very little effect on either the K^+ current or the Na^+ current. Test substances were applied *via* a perfusion pipette for a few seconds before, during and after each voltage pulse. Bath solution: ASW (see Fig. 3; drugs were added to this solution). 400K internal solution: 20 mmol l^{-1} KCl, 355 mmol l^{-1} potassium glutamate, 25 mmol l^{-1} KF, 10 mmol l^{-1} EGTA, 15 mmol l^{-1} Hepes.

TBA^+ also affected the shape of action potentials and induced hyperexcitability in current-clamped pyriform receptor cells. Fig. 6A,B compares membrane voltage responses to a 30 ms current pulse of +200 pA before (control) and during the puff application of 20 mmol l^{-1} TBA^+. The blocking of K^+ channels by TBA^+, as discussed above, increased the cell's excitability and facilitated a second AP during the current pulse. In addition, the AP was broadened in the presence of TBA^+ from a half-amplitude duration of 2.3 ms to 2.9 ms. A similar example of the effects of TBA^+ on another pyriform cell is shown in Fig. 6C,D. Such changes in the cell's excitability would presumably alter information encoded by the pattern of impulses passing from an olfactory receptor cell to the brain of a living squid.

Another behaviorally active chemical, 4-AP, is a well-known blocker of voltage-gated K^+ channels (Thompson, 1982; Rudy, 1988). Fig. 7A shows that, in a

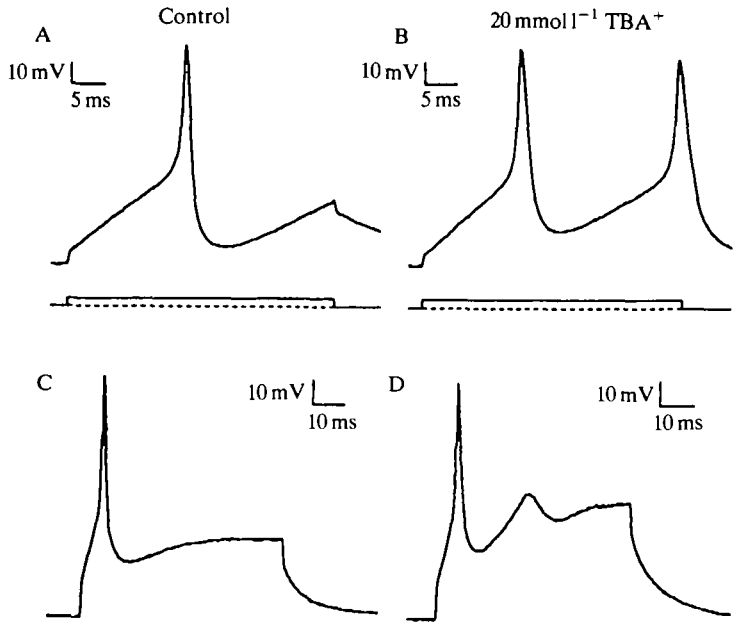

Fig. 6. 20 mmol l^{-1} TBA$^+$ affects excitability of current-clamped olfactory cells. (A,C) Control action potentials from two different pyriform receptor cells were elicited during a 30 ms (A) or 60 ms (C) current injection of 200 pA. (B,D) 20 mmol l^{-1} TBA$^+$ was applied from a perfusion pipette to each cell for several seconds before and during the matching current pulse. Bath solution: ASW (see Fig. 3). 400K internal solution: see Fig. 5.

pyriform receptor cell, approximately 50 % of the outward K^+ current during a voltage step to +30 mV is blocked by bath application of 5 mmol l^{-1} 4-AP. Inward Na^+ currents are not affected. A similar K^+-selective block by 4-AP is shown in Fig. 7C for a floriform cell.

A third type of channel blocker that caused escape behavior in squid is methadone. This tertiary amine was chosen because its effects on the ionic currents in squid GFL neurons had already been characterized (Horrigan, 1990). As was found in giant fiber lobe neurons, 500 μmol l^{-1} methadone almost completely blocks both Na^+ and K^+ currents in pyriform and floriform cells (Fig. 7B,D). These effects are readily reversible (not illustrated) and do not involve opiate receptors.

A well-known Na^+ channel blocker that did not elicit escape jetting in behavioral experiments was tetrodotoxin (TTX). In voltage-clamp studies, we found that 100–200 nmol l^{-1} TTX completely blocked Na^+ currents in both pyriform and floriform receptor cells without affecting K^+ currents (not illustrated). Thus, all the channel-blocking compounds that have proved to be active in behavioral experiments block K^+ channels when employed at the same concentrations. A subset of these (methadone and propyl paraben) blocks both K^+ and

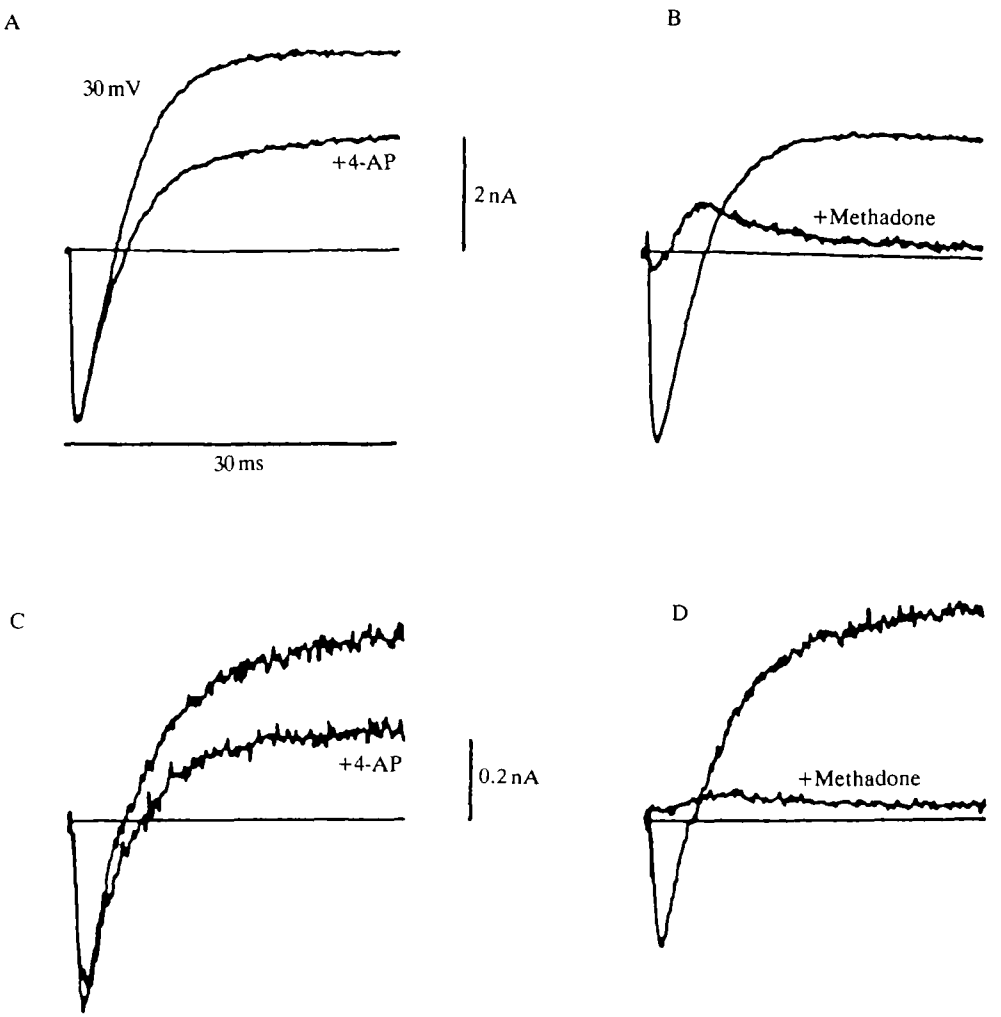

Fig. 7. 4-AP and methadone block K^+ currents in isolated olfactory receptor cells. (A,C) Superimposed current traces are illustrated for 30 ms pulses to +30 mV in the presence (+4-AP) and absence of 5 mmol l^{-1} 4-AP for a pyriform cell (A) and a floriform cell (C). (B,D) Currents recorded at +30 mV are shown in the presence (+Methadone) and absence of 500 μmol l^{-1} methadone for a pyriform cell (B) and a floriform cell (D). Bath solution: ASW (see Fig. 3; drugs added to this solution). 100K internal solution: see Fig. 3.

Na^+ channels, but TTX, which selectively blocks Na^+ currents, does not produce behavioral effects.

Effects of naturally occurring substances on electrical activity of receptor cells

Squid ink is a substance that squid encounter when they, or more likely fellow squid, have recently been alarmed. We found that a 1:20 dilution of squid ink

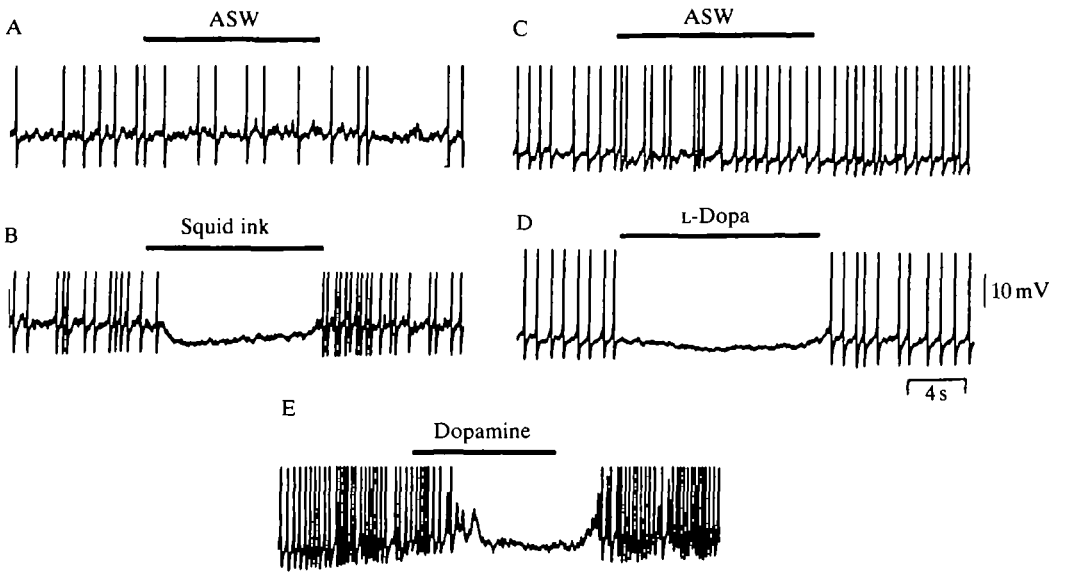

Fig. 8. Squid ink, L-Dopa and dopamine hyperpolarize the membrane and block action potentials in isolated pyriform receptor cells. (A) ASW was applied *via* a small perfusion pipette for the duration of the solid bar. The pipette was then rapidly removed from the bath. The peaks of the action potentials have been truncated. (B) Squid ink extract was applied in the same manner to the same cell. (C) A control puff application of ASW in a different cell. (D) 10 mmol l^{-1} L-Dopa was applied to the same cell as in C. (E) 50 μmol l^{-1} dopamine was applied to a different cell. Bath solution: ASW (see Fig. 3). 400K–nystatin internal solution: 20 mmol l^{-1} KCl, 355 mmol l^{-1} potassium glutamate, 25 mmol l^{-1} KF, 10 mmol l^{-1} EGTA, 15 mmol l^{-1} Hepes, 50 μg ml^{-1} nystatin.

caused escape jetting in behavioral experiments (Gilly and Lucero, 1992). In the following experiments, the nystatin patch recording method was used in an attempt to keep any second messenger systems as intact as possible (see Materials and methods). In these experiments, only current-clamp measurements were made, and the electrical resistance through the pipette and patch of membrane containing the nystatin pores was considerably higher than that required for good voltage-clamp control. Attempts to obtain the results to be described using conventional whole-cell recording techniques were unsuccessful.

Subtle changes in membrane potential are most easily observed when the cell is tonically firing near threshold, and the pattern of firing during a train of APs is a particularly sensitive indication of small hyperpolarizations. Thus, after a stable membrane potential had been obtained, the cell was routinely depolarized by injecting a steady current beyond threshold to approximately −35 mV, a level at which a tonic AP discharge occurred. A control 'puff' of ASW applied to the pyriform receptor cell had no effect on the action potential firing rate, as shown in Fig. 8A. In contrast, squid ink extract (see Materials and methods) reversibly

hyperpolarized the membrane potential by approximately 5 mV and inhibited AP firing (Fig. 8B).

Not all pyriform cells were responsive to ink application. For a cell to respond by inhibiting action potentials, it had to be capable of sustaining prolonged (1–2 min) tonic firing. Although 17 of the 25 cells tested were capable of tonic firing, only 11 of the 17 tonically active cells responded to ink. Many of the sensitive cells responded to repeated applications, but most became electrically leaky after the third or fourth trial.

Membrane resistance was monitored before, during and after application of ink (in experiments like that in Fig. 8B) by periodically delivering brief hyperpolarizing current pulses (−50 pA for 200 ms) through the patch pipette (data not shown). In such experiments, the response to ink was associated with a 28±4 % (N=3) decrease in membrane resistance. This decrease in membrane resistance was significantly different from the 1.5±0.6 % (N=3) decrease in membrane resistance associated with control application of 1 mmol l^{-1} blue no. 1 dye (independent t-test, $P<0.05$). Thus, it appears that K^+, or possibly Cl^-, channels are opening in response to squid ink and this serves to hyperpolarize the cell.

We have not been successful at detecting a membrane current associated with the application of squid ink under voltage-clamp conditions. However, in a pyriform cell with an average input resistance of 406 MΩ, an ink-induced hyperpolarization of 5 mV would correspond to a current as small as 12.5 pA. A current of this size was beyond the limit of resolution in our whole-cell recordings.

The pigment in squid ink is melanin, the precursor of which is L-Dopa (Fox and Crane, 1942). 1 mmol l^{-1} L-Dopa, like squid ink, elicited escape jetting in behavioral experiments (Gilly and Lucero, 1992). Similarly, 1–10 mmol l^{-1} L-Dopa mimicked the effect of squid ink in pyriform cells when puff-applied (Fig. 8D). This result was obtained in six of eight cells tested. As with squid ink, membrane resistance transiently decreased during the L-Dopa-induced hyperpolarization. There was no dramatic change in firing rate or membrane conductance during control application of ASW, as shown in Fig. 8C.

Preliminary studies show that 50 μmol l^{-1} dopamine also hyperpolarizes the membrane potential and inhibits action potential firing (Fig. 8E). The dopamine-induced hyperpolarization appears to develop more slowly and to persist for a longer time than the effect produced by ink or L-Dopa, but detailed comparisons are not yet possible. It seems likely, however, that L-Dopa or a compound derived from it plays a role in the hyperpolarization induced by squid ink.

Discussion

Resting membrane potentials of pyriform receptor cells, measured immediately after rupturing the cell membrane, averaged −58±1 mV and are similar to resting potentials in isolated olfactory cells from both vertebrates and invertebrates (Firestein and Werblin, 1987, −54 mV±8.2 mV, ±S.D.; Schmiedel-Jakob *et al.* 1989, −55.8±2.9 mV, ±S.E.). The resting potential of floriform receptor cells was

less negative, varying from −50 to −25 mV. Floriform cells were difficult to record from in current clamp because the resting membrane potential tended to fluctuate sporadically.

Voltage-clamp studies on isolated receptor cells showed that channel-blocking chemicals used in the behavioral studies could be divided into three classes: (1) those that block only K^+ channels, such as tetrabutylammonium (TBA^+), tetraethylammonium (TEA^+) and 4-aminopyridine (4-AP), (2) those that block K^+ and Na^+ channels, including methadone and propyl paraben, and (3) a strictly Na^+ channel blocker, TTX. It appears that the common underlying mechanism of transduction for the first two classes of compounds involves K^+ channel block and an increase in excitability of the receptor cell. Detection of TTX is not evident from our behavioral studies (Gilly and Lucero, 1992).

Block of K^+ currents changes the shape and frequency of action potentials in isolated olfactory receptor neurons and presumably these changes, upon reaching the brain of a living squid, initiate the series of events culminating in a powerful escape jet. At present we do not know the precise spatial distribution of K^+ channels in squid chemoreceptors, but presumably they exist in both the exposed apical region as well as the basolateral region, which gives rise to the axon. The exposure of the entire cell to K^+ channel blockers poses the potential problem that K^+ channel block is primarily affecting non-sensory pathways. However, the finding that externally acting chemicals, such as the membrane-impermeant quaternary ammonium ions, elicit escape responses, strongly suggests that at least some of a receptor cell's K^+ channels are located in the apical region that lies in direct contact with chemical stimuli in sea water (Gilly and Lucero, 1992). In this respect, squid olfactory receptors appear to be similar to vertebrate taste receptors in which signal transduction pathways include blockage of K^+ conductances to produce depolarizing receptor potentials (Kinnamon and Roper, 1988; Bigiani and Roper, 1991).

Some indirect evidence for localization of Na^+ channels to discrete regions on the squid receptor cell comes from experiments with TTX, a chemical that blocks Na^+ currents and action potentials in isolated squid olfactory cells. Inhibition of firing by TTX applied to a living animal presumably does not occur, because TTX does not induce escape responses. Squid ink and L-Dopa (which also block action potentials), in contrast, are potent stimulants that reliably induce escape responses in living squid (Gilly and Lucero, 1992). The lack of behavioral sensitivity to externally applied TTX suggests that most Na^+ channels are located in an area that does not come in direct contact with the external milieu. Thus, the bulk of the Na^+ channels appear to be localized to the basolateral, axonal pole of the neurons.

Evidence for the absence of voltage-gated Na^+ channels in dendritic regions of olfactory receptor cells exists in lobster (McClintock and Ache, 1989). However, unlike lobster, squid receptor cells appear to have voltage-gated Na^+ channels in the soma, because sizable Na^+ currents are still present even when there is little or no axonal remnant. In fact, cells with short axons or none at all were specifically selected for the present experiments to minimize space-clamp problems. Mapping

experiments on individual receptor cells would be useful in determining whether, as behavioral experiments suggest, Na^+ channels are absent from dendritic regions of squid olfactory receptors.

K^+ channel block as a mechanism of chemosensory transduction is undoubtedly only one of several mechanisms involved in squid olfaction. Squid ink appears to elicit escape jetting by a mechanism opposite to K^+ channel block. Squid ink suppresses activity in the isolated receptor cells by increasing membrane conductance to presumably K^+ or Cl^- and hyperpolarizing the cell's membrane potential. Although the only evidence for hyperpolarizing responses to odorants by vertebrate receptor cells was obtained in the mudpuppy (Dionne, 1990), recent work on lobster olfactory receptor cells shows an odor-activated K^+ conductance that reduces both the rate and the magnitude of an odor-activated depolarization and, thus, potentially modulates stimulus coding (Michel *et al.* 1991). Further studies with squid receptor cells will be necessary to determine both the selectivity of the ink-induced conductance increase and the extent to which it might modulate responses to depolarizing stimuli.

The major component of squid ink is melanin (Fox and Crane, 1942). L-Dopa, the precursor for melanin, is also found in squid ink (Jimbow *et al.* 1984) and elicits escape jetting in squid (Gilly and Lucero, 1992). In isolated olfactory receptor cells, L-Dopa and dopamine mimic the squid ink-induced suppression of action potentials. D_2 dopamine receptors may be localized in olfactory nerve terminals in the rat olfactory bulb (Boyson *et al.* 1986), and *in situ* hybridization studies suggest that olfactory receptor cells are capable of synthesizing dopamine receptors (Shipley *et al.* 1991). Although it is known that certain molluscan neurons express dopamine receptors and hyperpolarize when stimulated with dopamine (Walker, 1986), it remains to be seen whether the hyperpolarizing responses to squid ink and L-Dopa of olfactory neurons are the result of activation of a similar or novel dopaminergic transduction pathway.

We wish to thank Jimmy Lucero for performing the microdissection and tissue culture of the olfactory organ and Bruce Hopkins for providing the squid and scanning electron micrographs. This work was supported by the Office of Naval Research grant N0014-89-J-1744.

References

ARMSTRONG, C. M. AND BEZANILLA, F. (1974). Charge movement associated with the opening and closing of the activation gates of Na channels. *J. gen. Physiol.* **63**, 533–552.

BIGIANI, A. R. AND ROPER, S. D. (1991). Mediation of responses to calcium in taste cells by modulation of a potassium conductance. *Science* **252**, 126–128.

BOYSON, S. J. MCGONIGLE, P. AND MOLINOFF, P. B. (1986). Quantitative autoradiographic localization of the D_1 and D_2 subtypes of dopamine receptors in rat brain. *J. Neurosci.* **6**, 3177–3188.

BRISMAR, T. AND GILLY, W. F. (1987). Synthesis of sodium channels in the cell bodies of squid giant axons. *Proc. natn. Acad. Sci. U.S.A.* **84**, 1459–1463.

DIONNE, V. (1990). Excitatory and inhibitory responses induced by amino acids in isolated mudpuppy olfactory receptor neurons. *ACHEMS Abstr.* **12**, 50a.

EMERY, D. G. (1975). The histology and fine structure of the olfactory organ of the squid *Lolliguncula brevis* Blainville. *Tissue & Cell* **2**, 357–367.

FIRESTEIN S. AND WERBLIN, F. S. (1987). Gated currents in isolated olfactory receptor neurons of the larval tiger salamander. *Proc. natn. Acad. Sci. U.S.A.* **84**, 6292–6296.

FOX, D. L. AND CRANE, S. C. (1942). Concerning the pigments of the two-spotted octopus and the opalescent squid. *Biol Bull. mar. biol. Lab., Woods Hole* **82**, 284–291.

GILLY, W. F. AND BRISMAR, T. (1989). Properties of appropriately and inappropriately expressed sodium channels in squid giant axon and its somata. *J. Neurosci.* **9**, 1362–1374.

GILLY, W. F. AND LUCERO, M. T. (1992). Behavioral responses to chemical stimulation of the olfactory organ in the squid *Loligo opalescens*. *J. exp. Biol.* **162**, 209–229.

HAMILL, O. P., MARTY, A., NEHER, E., SAKMAN, B. AND SIGWORTH, F. J. (1981). Improved patch-clamp techniques for high-resolution current recording from cells and cell-free membrane patches. *Pflügers Arch.* **391**, 85–100.

HORN, R. AND MARTY, A. (1988). Muscarinic activation of ionic currents by a new whole cell recording method. *J. gen. Physiol.* **92**, 145–159.

HORRIGAN, F. T. (1990). Methadone block of neuronal K current. *Biophys. J.* **57**, 515a.

JIMBOW, K., MIYAKE, Y., HOMMA, K., YASUDA, K., IZUMI, Y., TSUTSUMI, A. AND ITO, S. (1984). Characterization of melanogenesis and morphogenesis of melanosomes by physicochemical properties of melanin and melanosomes in malignant melanoma. *Cancer Res.* **44**, 1128–1134.

KINNAMON, S. C. AND ROPER, S. D. (1988). Membrane properties of isolated mudpuppy taste cells. *J. gen. Physiol.* **91**, 351–371.

LLANO, I. AND BOOKMAN, R. J. (1986). Ionic conductances of squid giant fiber lobe neurons. *J. gen. Physiol.* **88**, 543–569.

LUCERO, M. T., HORRIGAN, F. T., LEVITT, J. L. AND GILLY, W. F. (1991). Chemoreceptive capabilities of the squid olfactory organ. *Biophys. J.* **59**, 184a.

MCCLINTOCK, T. S. AND ACHE, B. W. (1989). Ionic currents and ion channels of lobster olfactory receptor neurons. *J. gen. Physiol.* **94**, 1085–1099.

MESSENGER, J. B. (1979). The nervous system of *Loligo*. IV. The peduncle and olfactory lobes. *Phil. Trans. R. Soc. Lond.* B **285**, 275–309.

MICHEL, W. C., MCCLINTOCK, T. S. AND ACHE, B. W. (1991). Inhibition of lobster olfactory receptor cells by an odor-activated potassium conductance. *J. Neurophysiol.* **65**, 446–453.

RUDY, B. (1988). Diversity and ubiquity of K channels. *Neuroscience* **25**, 729–750.

SCHMIEDEL-JAKOB, I., ANDERSON, P. A. V. AND ACHE, B. W. (1989). Whole cell recording from lobster olfactory receptor cells: responses to current and odor stimulation. *J. Neurophysiol.* **61**, 994–1000.

SHIPLEY, M. T., NICKELL, W. T., NORMAN, A. B. AND GERFEN, C. (1991). Localization of D_2 dopamine receptor messenger RNA in primary olfactory neurons. *ACHEMS Abstr.* **13**, 108a.

THOMPSON, S. (1982). Aminopyridine block of transient potassium current. *J. gen. Physiol.* **80**, 1–18.

WALKER, R. J. (1986). Transmitters and modulators. In *The Mollusca*, vol. 9 (ed. A. O. D. Willows), pp. 314–347. New York, London: Academic Press, Inc.

WATKINSON, G. (1909). Untersuchungen über die sogenannten Geruchsorgane der cephaloden. *Jena Z. Naturw.* **44**, 353–414.

WELLS, M. J. AND WELLS, J. (1959). Hormonal control of sexual maturity in *Octopus*. *J. exp. Biol.* **36**, 1–33.

WILDENBURG, G. AND FIORONI, P. (1990). Ultrastructure of the olfactory organ during embryonic development and at the hatchling stage of *Loligo vulgaris* Lam. (Cephalopoda). *J. Ceph. Biol.* **1**, 56–70.